Direct measurements of the effects of salt and surfactant on interaction forces between colloidal particles at water-oil interfaces

Bum Jun Park, John P. Pantina, and Eric M. Furst*
Department of Chemical Engineering, University of Delaware
Newark, Delaware 19716, USA

Martin Oettel
Institut für Physik, Johannes-Gutenberg-Universität Mainz
WA 331 55099 Mainz, Germany

Sven Reynaert and Jan Vermant†
Department of Chemical Engineering, Katholieke Universiteit Leuven
W. de Croylaan 46, B-3001 Leuven, Belgium

*furst@udel.edu
†jan.vermant@cit.kuleuven.be

Abstract

The forces between colloidal particles at a decane-water interface, in the presence of low concentrations of a monovalent salt (NaCl) and of the surfactant sodium dodecylsulfate (SDS) in the aqueous subphase, have been studied using laser tweezers. In the absence of electrolyte and surfactant, particle interactions exhibit a long-range repulsion, yet the variation of the interaction for different particle pairs is found to be considerable. Averaging over several particle pairs was hence found to be necessary to obtain reliable assessment of the effects of salt and surfactant. It has previously been suggested that the repulsion is consistent with electrostatic interactions between a small number of dissociated charges in the oil phase, leading to a decay with distance to the power -4 and an absence of any effect of electrolyte concentration. However, the present work demonstrates that increasing the electrolyte concentration does yield, on average, a reduction of the magnitude of the interaction force with electrolyte concentration. This implies that charges on the water side also contribute significantly to the electrostatic interactions. An increase in the concentration of SDS leads to a similar decrease of the interaction force. Moreover the repulsion at fixed SDS concentrations decreases over longer times. Finally, measurements of three-body interactions provide insight into the anisotropic nature of the interactions. The unique time-dependent and anisotropic interactions between particles at the oil-water interface allow tailoring of the aggregation kinetics and structure of the suspension structure.

Introduction

The behavior of colloidal particles at liquid interfaces is of great practical importance [see ref. [1] for a recent review]. For example, particles stabilized emulsions and foams can be produced [2, 3, 4], which are encountered in both established and emerging areas of technology. Examples include froth flotation or ice-cream production, as well colloidal self-assembly and the production of colloidal capsules (colloidosomes) [5]. Exploiting properties of particles at interfaces can also be used to create crystalline assemblies of varying form [6] or colloidal microcrystals of well defined geometry [7]. As for all applications where colloidal materials are being processed, there is a need to understand the colloidal interactions in order to have control over the structure, and hence the properties. For example, the most efficient stabilization of Pickering emulsions will probably be achieved by a relatively low surface coverage and weakly aggregated structure at the droplet interfaces [8, 9]. Planar monolayers of particles with controlled interactions also enable fundamental studies of colloid physics, such as crystal melting [10], aggregation [11, 12, 13, 14], packing and self-assembly of non-spherical particles [15, 16] and even elucidate the effects of shear or extensional flow on the microstructure of suspensions [17, 18]. In all cases, predictive control over the generated structures is needed, necessitating a detailed understanding of the colloidal interactions.

Despite the thorough understanding of colloid and surface forces developed over the past century [19, 20], the presence of an interface adds significant complexity to the colloidal interactions. A first illustration hereof is the remarkable stability of two-dimensional colloidal crystals when the ionic strength of the aqueous phase is increased [12, 21, 14]. Monolayers of initially charged polystyrene latex beads spread on an aqueous subphase containing as much as 0.5 M of a monovalent or divalent salt were observed to be stable

for several days before aggregation set in [12, 14], whereas the bulk system aggregates on the timescale of minutes. Secondly, there is also a strong dependence on how monolayers are prepared [23]. For example, when particles are first spread onto a virgin interface, and salt is added to the aqueous subphase slowly after that, the aggregation proceeds as expected, after the long induction process mentioned. Yet, particles spread onto an aqueous subphase already containing the salt can result in a monolayer where crystalline patches and dense aggregates coexist [14]. Finally, probably the most remarkable illustration of the complexity of the interaction forces is the occurrence of so-called mesoscale structures. At low surface coverage, fascinating patterns can be readily observed, including voids, line patterns, soap froths and particle loops [24, 25, 26, 27]. They are consistent with the presence of an attractive, secondary minimum in the intercolloidal potential at distances spanning several particle diameters, and with a well depth on the order of thermal energy kT, although it has also been suggested that they are a consequence of like-charge attractions [28].

There appear to be two main causes for this increased complexity. First, the repulsive electrostatic interaction occurs through two media with different values of the dielectric constants. Second, the presence of charged particles can create distortions of the interface, which can give rise to (predominantly attractive) lateral capillary interactions. We will briefly review the understanding of both classes of interactions.

Compared to similar particles in a bulk liquid, the electrostatic repulsion between charged particles is enhanced at a water-low dielectric medium interface, as was recognized early on by Pieranski [30]. At the interface, a particle has an asymmetric counterion distribution which results in a dipole-dipole interaction through the phase of low dielectric constant. It has been shown that the corresponding interaction is repulsive and long-

ranged. The force decays inversely with the fourth power of the separation between the dipoles, and depends strongly on electrolyte concentration, through the Debye screening length κ^{-1} [32, 33],

$$F_E = \frac{3\varepsilon_{oil}}{2\pi\varepsilon_0\varepsilon_W^2} \cdot \frac{q^2\kappa^{-2}}{r^4} \qquad . \tag{1}$$

The permittivity of free space and the relative dielectric constant of water and oil are given by ε_0, ε_W and ε_{oil}, respectively. Because only the particle surface charges within a distance κ^{-1} from the three-phase contact line contribute to the equivalent point charge q, Aveyard et al. suggested that the force depends on κ^{-4} [31]. The relative independence of two-dimensional colloidal crystals to the electrolyte concentration which is experimentally observed [12, 21], suggests that the Hurd model does not adequately describe the electrostatic interaction. A recent explanation for a weaker dependence on κ^{-1} is that charge renormalization is important due to the high surface charge density [22]. This problem has been studied by solving Maxwell's equation in the oil phase and the Poisson-Boltzmann equation in the water phase, assuming constant charge density σ on the colloid surface exposed to water. The dipole character of the interaction is retained, and far enough from the particle surface one recovers eq. 1, but q needs to be replaced by an effective charge $q_{eff} = q\,g$. For a particle of radius R, the charge renormalization function g depends primarily on a reduced inverse screening length $\kappa^* = \kappa R$, a reduced charge density $\sigma^* = \sigma(eR)/(kT\,\varepsilon_0\varepsilon_W)$ and, to a minor extent, also on the ratio of the dielectric constants between the different media and on the geometry through the contact angle θ (e is the elementary charge). For sufficiently high surface charge densities the scaling of F_E with the screening length becomes [22]:

$$F_E \propto \ln^2 \frac{\sigma^*}{\kappa^*} \tag{2}$$

which yields a weak power–law dependency of $\kappa^{-0.8\cdots-0.4}$ for physical charge densities $\sigma = 1\ldots10\ \mu\mathrm{C/cm}^2$ ($\sigma^* \approx 800\ldots8000$), which clearly is different from the linear results.

Alternatively, it has been suggested that 'monopolar' Coulomb repulsive interactions must also be taken into account. Aveyard *et al.* [21] hypothesized that a small number of unscreened surface electric charges, possibly arising from dissociated surface groups, are stabilized by water trapped on the rough particle surface. The force acting between the particles can be calculated as a function of the interparticle distance, using Stillingers approach [21, 23], where the charges in the oil phase are represented by a point charge q_{oil} located at a distance above the oil-water interface. For sufficiently large particle separations, this force (labeled F_{Eo}) has the characteristic dependence of a dipole-dipole interaction on interparticle distance (r) [21, 31]:

$$F_{Eo} \approx \frac{q_{oil}^2}{4\pi\varepsilon_{oil}\varepsilon_0}\left[\frac{1}{r^2} - \frac{r}{(4\zeta^2 + r^2)^{3/2}}\right] \qquad , \tag{3}$$

with ζ being the distance of an equivalent point charge over the dimensions of the particle,

$$\zeta = R\frac{(3 - \cos\theta)}{2} \qquad , \tag{4}$$

where θ is the contact angle and R the particle radius. The charge q_{oil} is given by the product of the particle surface area immersed in the oil, the surface charge density σ and the fractional degree of dissociation, α_{oil}, of the ionizable groups at the oil-particle interface:

$$q_{oil} = 2\pi R^2(1 - \cos\theta) \cdot \sigma \cdot \alpha_{oil} \qquad . \tag{5}$$

The expected force contribution from this 'oil side' effect is independent of κ. The limit for $(r/\zeta)^2 \gg 1$ of Eqn.3 is [21, 31]

$$F_{Eo} \sim \frac{3q^2}{8\pi\varepsilon_{oil}\varepsilon_0}\frac{\zeta^2}{r^4}. \tag{6}$$

Direct measurements using optical tweezers confirmed the r^{-4} dependence, and it was shown that the measured force did not change significantly when 0.1mM of NaCl was added

to the aqueous phase. However, some issues remain, as the data set is rather limited and the inferred degree of dissociation that produces q_{oil}, ranges from 0.033% [31] to 1% [21], for the same type of particles, depending on the measurement technique, i.e. pair interaction measurements using laser tweezers versus bulk surface pressure isotherms. Molecular dynamics simulations suggest that the combination of the short-range dipole-dipole interactions and long-range charge-charge repulsions adequately describes the experimentally observed isotherms, provided α equals 0.4% [34], which is an order of magnitude above the results from the direct tweezer measurements.

Considering the attractive contributions, a dominant feature of colloidal suspensions at interfaces is the occurrence of lateral capillary forces. They appear when the presence of particles at a fluid phase boundary causes perturbations in the interfacial shape, which subsequently overlap [36]. For particles which cause similar interfacial deformations, i.e. both downward or both upward, the lateral capillary forces are attractive in nature. Assuming a superposition of the interfacial deformation profiles, Kralchevsky and Nagayama [35] calculated the interaction force when gravity is the determining force. For the particles studied in the present work, these gravitational forces are small ($\mathcal{O}[10^{-11}\mathrm{N}]$). More importantly, the dipolar electric field of the particles can also create a local force imbalance due to the Maxwell stress tensor, which can lead to electro-capillary interactions and medium ranged flotation-like forces [37, 38]. The electro-capillary force scales like

$$F_{cap} \sim -F_E \epsilon_F \qquad . \tag{7}$$

Hence, it is influenced by the same factors as the electrostatic force, but has an additional prefactor ϵ_F, which is given by the ratio of the total electrostatic force acting on the colloid and the surface tension force scale γR [37]. The magnitude of the electro-capillary force hence depends on the ratio of the total (vertical) electrostatic force acting on the colloid

to γR. Finally, capillary interactions depend on the shape of the meniscus, aspects such as asperities on the particle surface, particle or agglomerate shape. The interaction can be repulsive or attractive depending on the relative orientations of the interface deformations. This also implies that when doublets or irregular aggregates are formed with possibly complex undulating contact lines, the resulting capillary interactions will no longer be isotropic [36, 40, 41].

The aim of the present work is to investigate the control of colloidal interactions by the addition of small amounts of surfactant or salt to the aqueous subphase. Detailed measurements of the effect of electrolyte concentration should shed light on the importance of contributions of the charges on the oil and water sides to the electrostatic interaction force. The study of the effect of changing surfactant concentration is motivated by earlier observations that small amounts of either anionic or cationic surfactants lead to an efficient destabilization of the monolayer [29, 14]. Adding ionic surfactants will affect the screening length, the interfacial tension, but also the wetting conditions. In the present work, direct measurements of the effect on the overall interaction force are presented. The time-dependence of the inetercation force as well as the spatial anisotropy of the capillary interactions will be investigated and its role in structure formation will be measured in detail.

Materials and Methods

An oil-water interface was created using n-decane (Acros Organics, 99+%) and deionized water. Prior to use, polar components were removed from the decane using an adsorption onto aluminiumoxide powder (Acros Chemical, acidic activated, particle size 100-500μm). To modify the wetting properties and dielectric properties of the aqueous subphase small amounts of an ionic surfactant, sodium dodecylsuplhate (SDS, Sigma Aldrich 98+%), some-

times in combination with a monovalent salt (NaCl), were used. Monodisperse, charge stabilized polystyrene particles (9.1 μC/cm^2 and 3.1$\pm$0.2μm diameter) were obtained from Interfacial Dynamics Corporation. The charge is a result of the presence of sulfate groups at the particle surface.

Particle monolayers at the oil water interface are prepared according to the procedure outlined in Reynaert et al. [14]. A stable colloid monolayer is first prepared, and subsequently, salt or surfactant are carefully added to the aqueous subphase, without going through the oil phase, in a specially designed fluid cell to accommodate the short working distance of the microscope objective (i.e. a 200μm working distance for the 40$\times$ water immersion objective) required in the optical tweezer experiments.

Two experimental cells were used, as shown in Figure 1. The first experimental cell in fig. 1.a consists of an inner and outer cylinder made of aluminum. The inner cylinder is held by a micrometer, while the outer cylinder is attached to a 40mm circular No. 1.5 coverglass (Fisherbrand) using a fast curing UV epoxy (Norland Products, NOA 81). A teflon ring is inserted into the bottom of the inner cylinder in order to pin the contact line of the oil-water interface. Decane is placed in the cell first, achieving hydrostatic equilibrium between the inner and outer cylinder, and water is added to the inner cylinder. The height of the inner cylinder is adjusted to by raising or lowering it with the micrometer. Using the height adjustment along with the addition or removal of decane and water, ensures a flat interface.

The second experimental cell, as shown in Figure 1.b is built using two concentric glass rings (height of 1cm, outer diameter 39mm and 18mm, respectively, and a wall thickness of 1 mm), confining the oil-water interface within the inner ring. Again, the rings are

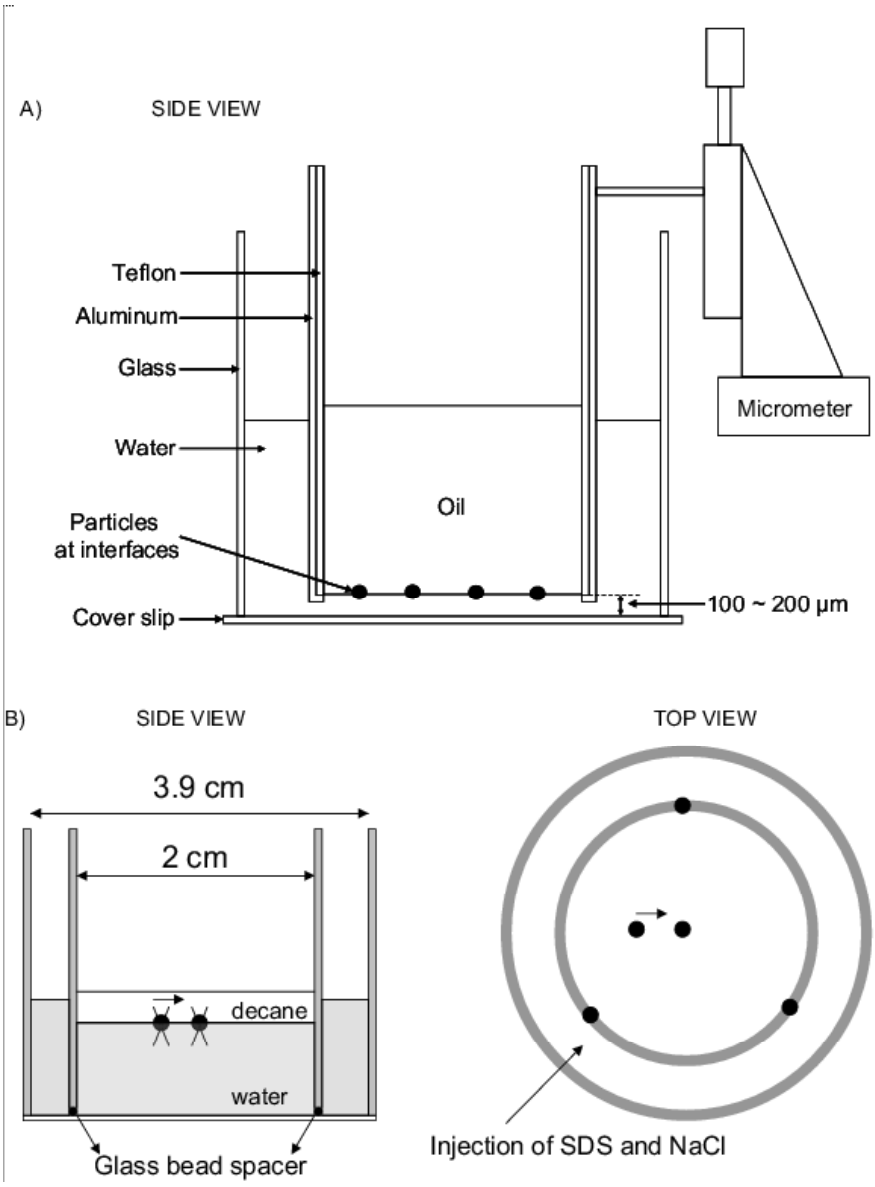

Figure 1: Experimental cells used for the optical tweezer experiments (a) Aluminium cell (b) Glass cell. See text.

attached to a 40mm circular No. 1.5 coverglass (Fisherbrand) using a fast curing UV epoxy (Norland Products, NOA 81). The outer ring is completely sealed to prevent any fluid leaks; however, a three-point attachment using 200μm glass beads as spacers between the inner ring and the coverglass are used. This enables the system to achieve hydrostatic equilibrium, thus providing control over the water layer by extracting water from or adding

water to the outer ring. In both experimental setups, all glassware is fire treated using a propane torch immediately before constructing the cell. This reduces the water-glass contact angle to below 15°, achieving good wetting conditions for the water layer.

The optical tweezer setup used is described in greater detail in Pantina and Furst [42]. Two methods were used in this study to measure forces with the optical traps. To calibrate the trapping force of the tweezers, particles were held at the interface and subjected to drag forces by translating the microscope stage at constant velocities, U. The displacement of the particle from the center of the optical trap is measured as a function of the Stokes drag force $F_S = 6\pi a \eta_{\text{eff}} U$, where the effective viscosity depends on both phases, $\eta_{\text{eff}} = [\eta_{oil}(1 - \cos\theta) + \eta_{water}(1 + \cos\theta)]/2$. This provides a calibration of the trap force profile and maximum trapping force.

An alternative method was used in some cases, in which the particle response to a sinusoidal oscillation of the optical trap is characterized. This method can better adapt to situations in which the curvature of the oil-water meniscus is significant, and dragging the particle at constant velocity is not feasible. At low frequencies, the particle is trapped and follows the beam. When the frequency of the oscillation is increased, the increasing viscous drag force acting on the particle causes it to leave the trap. Using the calculations from Faucheux et al. [43] the calibration constants can be obtained from the frequency at which the system transitions from "phase lock" to "phase slip". In all experiments, it was verified that measurements of the interaction forces where independent of the laser intensity. This implies that the optical tweezers are not exerting a net force on the particles. If a possible vertical net force were strong enough, attractive long-ranged forces should appear in the force measurements [37].

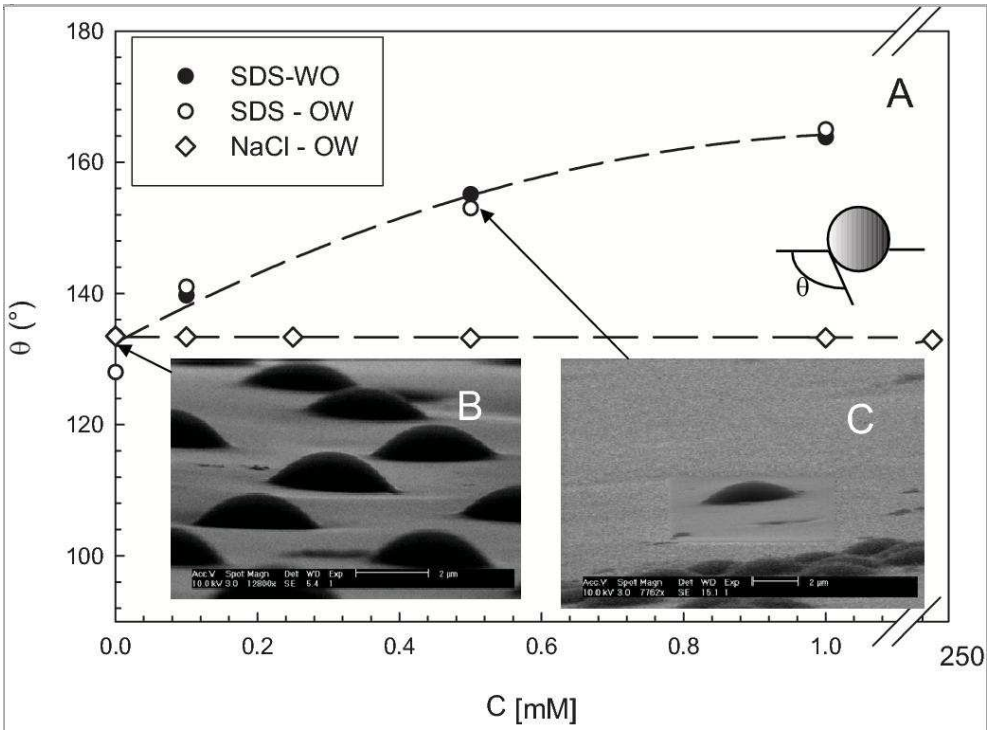

Figure 2: Effect of small amounts SDS and NaCl concentration on the contact angle on a polystyrene cast film for water-oil (WO) and oil-water (OW) interfaces (B) SEM image of gel trapped particles originally at a water-decane interface. (C) SEM image of a gel particle trapped originally at an oil-(water+0.5mM SDS) interface.

The contact angle θ of the particles at the oil water interface is measured using two independent methods. First, a film is cast of the PS particles dissolved in chloroform. A water droplet is subsequently gently placed on the PS film, and a decane environment is then generated around the droplet. A goniometer (CAM 200, KSV instruments) is used to measure θ. To check for contact line hysteresis, some measurements were also performed on the reverse system of a decane droplet in a water environment. The results (from ref. [14]) are given in figure 2. The contact angle increases as SDS is added, i.e. particles are pushed into the oil-phase. Becasue casting of the PS films may mead to slight differences in surface chemistry and changes in the wetting properties, we also used the so-called gel trapping technique of Paunov [44] to verify our results. The particles are spread at the oil-water

surface and the water phase is gelled using a nonadsorbing polysaccharide. The particle monolayer trapped on the surface of the gel is then replicated using a PDMS-elastomer. The particles, now embedded within the PDMS surface, are imaged with high resolution SEM (Philips XL300FEG-ESEM). Fitting the contour of the particles to a sphere gives information on the position and the particle contact angle at the air-water or the oil-water interface. Typical micrographs for a water-decane interface are given in the insert of figure 2(B). The SEM image for a subphase containing 0.5mM SDS is shown in figure 2(C). The reduction of the exposed particle surface is consistent with the particle being pushed into the oil phase. The value of the contact angle can be obtained by measuring the height above the interface and dividing it by the radius at the plane of intersection. The value obtained for the particle at the water- decane interphase is $118 \pm 2\,^{\circ}$ and for the system water(+ 0,5 mM SDS)- decane : $142 \pm 2\,^{\circ}$. These values are consistent with those observed from the cast films, the small differences being attributed to the presence of gellan in the aqueous phase. As expected in this range of concentrations, adding salt has a only a very limited effect on the contact angle, a small decrease is observed in the case film experiments, on the order of one degree, at the highest concentration studied (250mM).

Results and Discussion

Pair interaction

Effect of NaCl

Two particles are trapped at a sufficiently wide initial separation such that the repulsive interaction between the particles is weak. One particle is then moved step-wise to smaller separations. The displacement of the stationary particle is monitored in its optical trap. Using the calibrated trap stiffness, the force at a number of separations can be easily found in a manner analogous to the spring displacement in an AFM or surface forces apparatus.

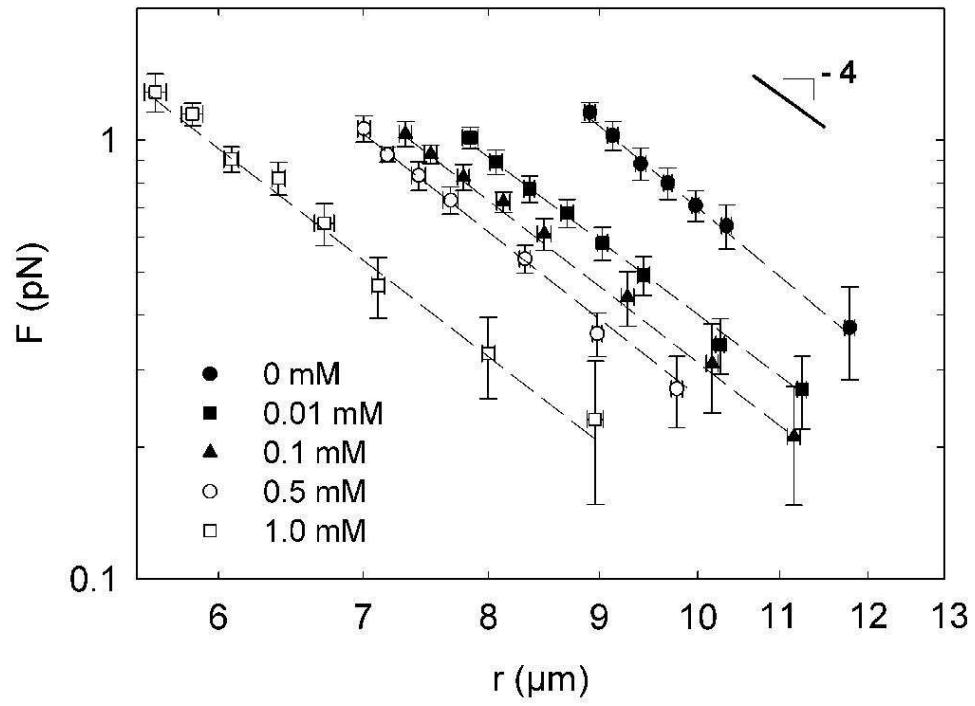

Figure 3: Measurement of the pair interaction between PS particles at the decane-water interface for different concentrations of NaCl in the subphase, approximately one hour after the monolayer was prepared.

Figure 3 shows the force profile measured for the pure water-decane interface and at four different NaCl concentrations, one hour after preparing the monolayer. Four aspects can be deduced. In agreement with the earlier observations of Aveyard et al [31], the force is repulsive, and is observed to scale as r^{-4}. Secondly, the force is found to be small, even somewhat smaller than the force values obtained by Aveyard et al. [31] using tweezers, but especially more than three orders of magnitude smaller than the values inferred from surface pressure area isotherms using a Wilhelmy plate and balance [29]. If the interaction as measured by the tweezer would be attributed to charges in the oil phase, this would correspond to a degree of dissociation smaller than 0.01%. The tweezer experiments were carefully checked for artefacts, using different particle arrangements, and even utilizing

multiple particles, e.g. placed on a hexagon, with a particle in the center. Nonetheless, on average, consistent values were always obtained. Most probably, the indirect Wilhelmy technique is less reliable for the particle laden interfaces. The Wilhelmy technique assumes that only a monolayer of particles, with the same structural arrangements as at the interface, stick to the plate and transmit the force. Changes in both the interaction force and the local structural arrangements may be caused by particle adsorption onto the plate, which may be complicated by the local curvature of the interface. Gel trapping measurements revealed slightly denser packed structures close to the Wilhelmy plate, and a corresponding enhancement of the electrostatic force is subsequently measured by the plate. This suggests that interpreting pressure-area isotherms obtained with the Wilhelmy technique in terms of the pair interaction should be handled with care. A third observation from the data in figure 3 is that the dependence on particle separation is also conserved for the systems containing salt in the subphase. And finally, it is shown that increasing the electrolyte concentration in the subphase significantly decreases the magnitude of the repulsive interactions. This is true *on average*; however, significant heterogeneity in the pair interactions are observed, depending on the particle pairs used in the force measurements, as discussed below. The error bars mainly reflect this variation on the measured interaction force.

To evaluate the presence of any time dependence, the rate of change in the repulsive particle interaction is measured. Figure 4 shows the force for several particle pairs at three different concentrations. For times up to three hours, no measurable change occurrs in the interaction force, either for the pure system, or for the systems containing salt in the subphase. Note, however, that the pair interactions exhibit significant variability under the same conditions. The force differs by as much as a factor 2. This could be due to a local surface charge inhomogeneity at the particle surfaces which could cause variations in

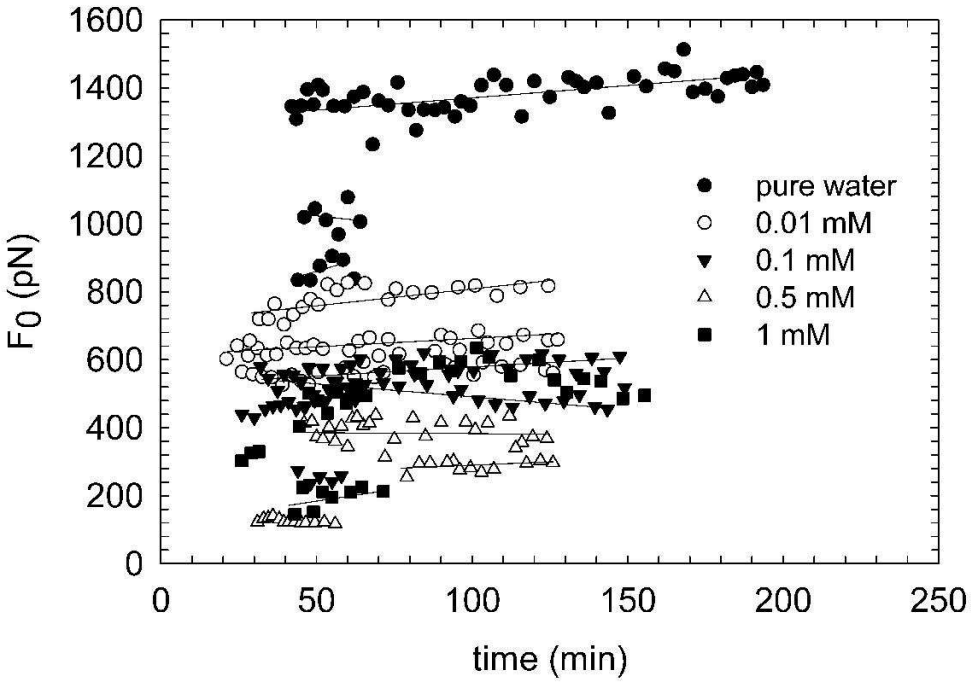

Figure 4: Typical measurements of the force between PS particles at the decane-water interface for pure water and three concentrations of NaCl in the subphase. F_0 is the amplitude of the dipole force parametrization $F(r) = F_0\,(R/r)^4$.

the repulsive part [28], or due to effects of nanoscale particle roughness or effects of the charge inhomogeneity on the homogeneity of the wetting which would lead to an attractive force of considerable magnitude [40].

Effect of SDS

SDS was added at concentrations well below its CMC to the subphase. Apart from changing the screening length in water by acting as an electrolyte, SDS also changes the wetting properties, and the particle is pushed further into the oil phase due to the change in the contact angle, as demonstrated in figure 2. When SDS is slowly added to the subphase and one assumes the charges on the oil side to stay the same, the effect of surfactant on the interaction forces should yield insight into the question of whether charges on the oil side

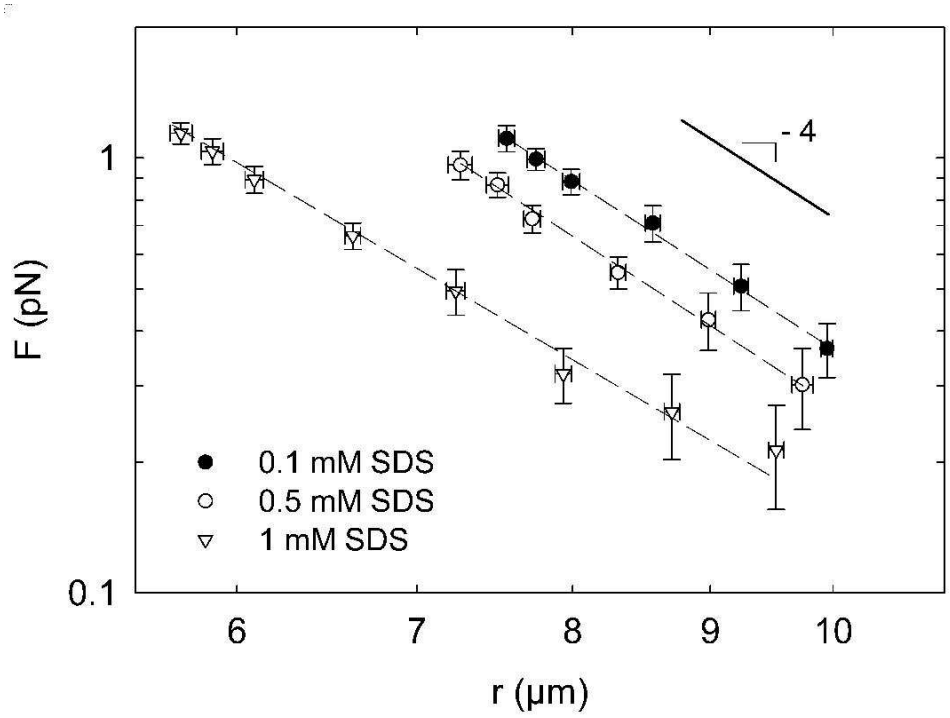

Figure 5: Measurement of the pair interaction between PS particles at the decane-water interface for different concentrations of SDS in the subphase, approximately one hour after the monolayer was prepared.

or on the water side dominate the repulsive forces. When the electrostatic forces on the oil side dominate, the interaction force should increase, the particles are pushed further in the oil phase (fig.2), increasing both the area exposed to the oil and the height above the interface. A decrease is expected when the water-side electrostatic forces dominate as the exposed area is decreased and the screening length increases because of the ionic nature of the surfactant. Figure 5 shows the force profile measured at three different SDS concentrations approximately one hour after preparing the monolayer. Similar to the addition of small amounts of NaCl, increasing the SDS concentration in the subphase decreases the magnitude of the repulsive interactions. Again, this is true only on average, as significant heterogeneity is also present here. As the repulsive interaction decreases at higher SDS concentrations, the repulsion softens, shown by the slight decrease in the scaling exponent

with particle separation. This suggests that a long-range attraction begins to play a role as particles come into closer separations.

Whereas the results above indicate that initial electrostatic repulsion remains significant, earlier studies showed that surfactants can completely *de*stabilize an initially crystalline monolayer [29, 14], albeit sometimes after very long incubation times. Therefore, the time dependence of the pair interaction was also investigated. Using a similar approach as in figure 5, the interaction force as a function of separation was monitored at different time intervals after preparation of the monolayer, as shown in figure 6. It is observed that the repulsion between the particles becomes weaker with time.

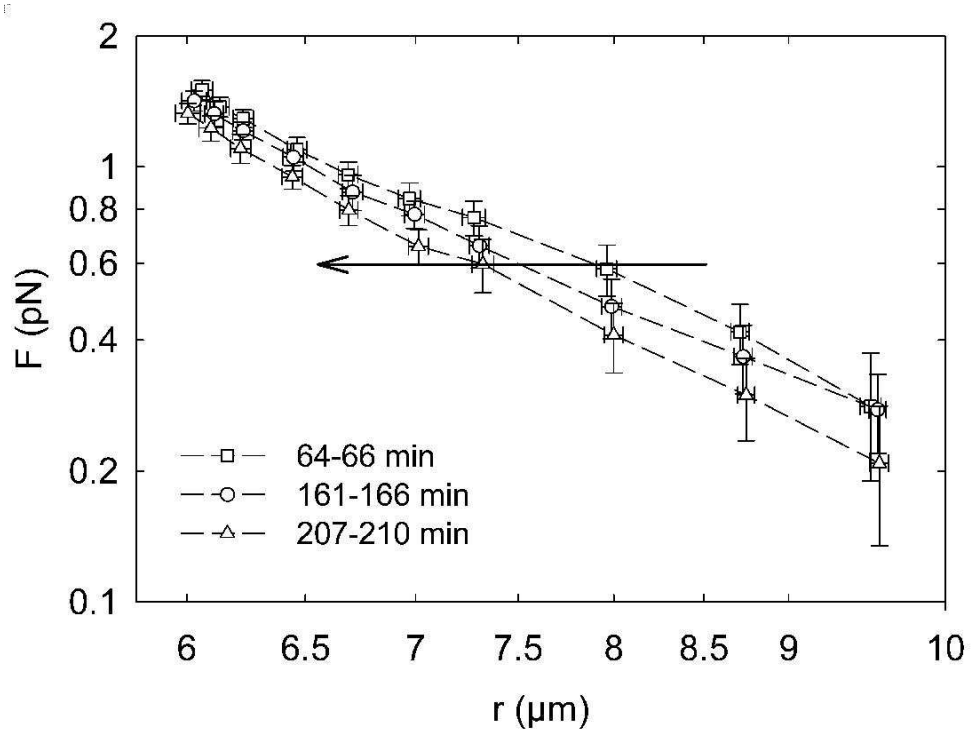

Figure 6: Comparison of the interaction force for a subphase containing 0.1 mM SDS at different times after preparation of the monolayer.

To examine the time dependence further, the rate of change in the repulsive particle interaction was measured. Figure 6 shows the force between particle pairs for 0.1mM SDS at three time intervals over the span of one to 3.5 hours. Over this period, the repulsion is observed to decrease. Note, however, that particle pairs again exhibit significant variability under the same conditions. Nonetheless, the average dependence on surfactant concentration shows a decreasing repulsion as the amount of surfactant in the subphase increases (figure 6). A possible explanation of the time dependence of the repulsive interactions is that the concentration of adsorbed SDS molecules on the oil-water interface changes with time, which would change θ. To rule out this possibility, the time dependence of the contact angle on flat substrates was measured for the oil-water interface with 0.1mM and 0.5mM SDS added to the aqueous phase. The contact angle was found to be constant for the case when 0.1mM was added to the subphase over a 25 minute time period, while θ was found to fluctuate approximately 4° over a 75 minute time period when 0.5 mM SDS was added. However, fitting our constant force measurements at $c_{SDS} = 0.5$mM using the Aveyard *et al.* model assuming a constant oil dielectric constant requires a change in θ of more than 15° over one hour. This is larger than the range of change observed using direct contact angle experiments on planar films.

The reasons for the slow time evolution in presence of SDS are not completely understood. The process is too slow to be related to a diffusion phenomenon of ions across the surface. One possibility is that surface hydrolysis of the SDS is taking place [45, 46], leading to the formation of dodecan-1-ol from the hydrolysis of SDS. This will change the adsorption of SDS onto the particles [46] and may affect the local composition near the interface, which has complex dynamics [47]. In all, the experimental results show that the electrostatic interaction becomes effectively more screened as time proceeds.

Effect of salt and SDS

Plotting the force after the addition of NaCl to the subphase, as a function of the Debye screening length κ^{-1}, the predictions of the different theoretical approaches for the electrostatic contribution with respect to the dependency on screening length can be evaluated. The inverse screening length was calculated from

$$\kappa = \sqrt{\frac{1000e^2 N_A}{\epsilon_W \epsilon_0 k_B T} 2I} \qquad , \tag{8}$$

where I is the ionic strength of the electrolyte, ϵ_0 is the permittivity of free space, k_B is the Boltzmann's constant, T is the temperature, N_A is Avogadro's Number and e is the elementary charge. For the pure water an ionic strength of 10^{-6}M was estimated, based on conductivity measurements. Figure 7 shows the force as a function of κ^{-1}. A weak, power law dependence of the magnitude of the force on the inverse screening length is observed with an exponent of 0.43±0.04. This can be compared to equation 2 using κR and $\sigma^* = \sigma(eR)/k_B T \epsilon_0 \epsilon_w$, where $\sigma^* = 7751$. For a pre-factor of 15.8, the resulting predictions from the charge renormalization theory [22] are in good agreement with the experimental values shown in figure 7. Interestingly, when treating SDS as a 1:1 electrolyte, a very similar dependence is observed, suggesting that the primary effect of SDS is to act as an electrolyte, although the change in the wetting properties could also play a significant role. As the particles are pushed further into the oil phase, less charged surface area remains in contact with the water.

Finally, it should be noted that the *combined* effect of salt and SDS on the interaction between two particles seems to be more complex. In the presence of both SDS and salt, aggregation is readily induced when particles are brought together, even at the lowest laser powers. For example, figure 8 shows the force profile for the combination of 0.1 mM SDS and 0.25 M NaCl at 108 minutes after spreading the particles. The range and magnitude

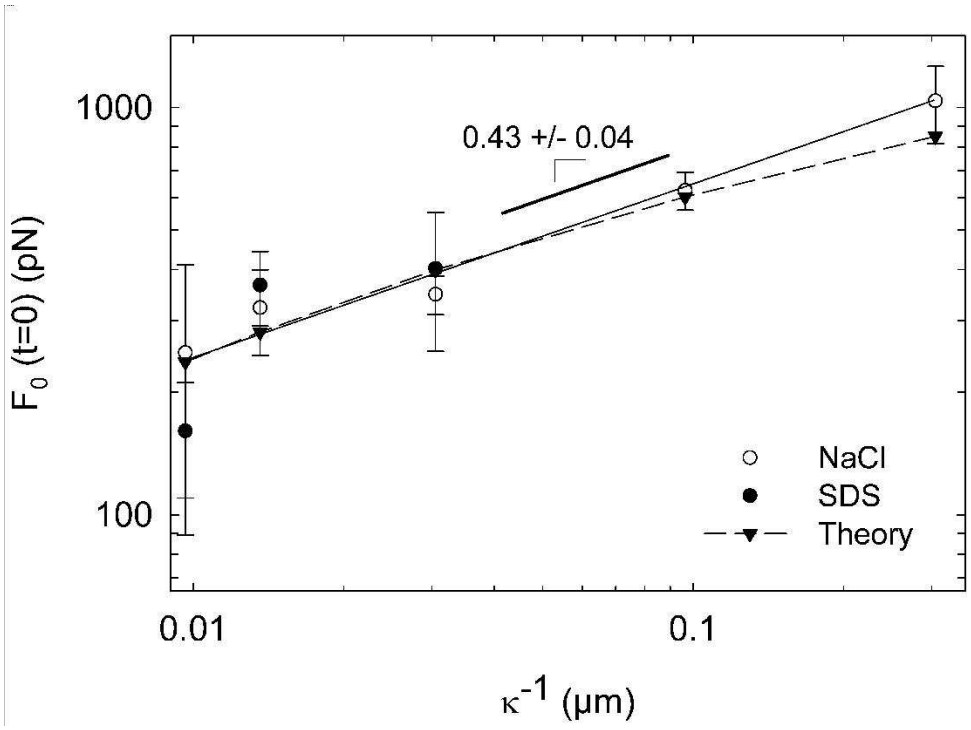

Figure 7: Effect of changing the Debye screening length on the interaction force for systems containing NaCl or SDS. F_0 is the amplitude of the dipole force parametrization $F(r) = F_0\,(R/r)^4$. The experimental results are compared with the expected dependence of the charge renormalization theory (cf. equation 2) [22]. The solid line is a power-law fit to the experimental data with a scaling exponent of 0.43±0.04.

of the repulsive interaction is lower than measurements with SDS alone, and the power-law exhibits a weaker scaling exponent. Therefore, the addition of salt further decreases the magnitude and scaling behavior of the far-field repulsion. In addition, the particles jump into a weak attractive minimum in the near-field, and exhibit a pull-out force with no hysteresis in the far-field interaction. This observation rationalizes earlier findings that combinations of salt and SDS lead to a more efficient destabilization of the 2D suspensions, whereas salt alone results in slow aggregation kinetics [14].

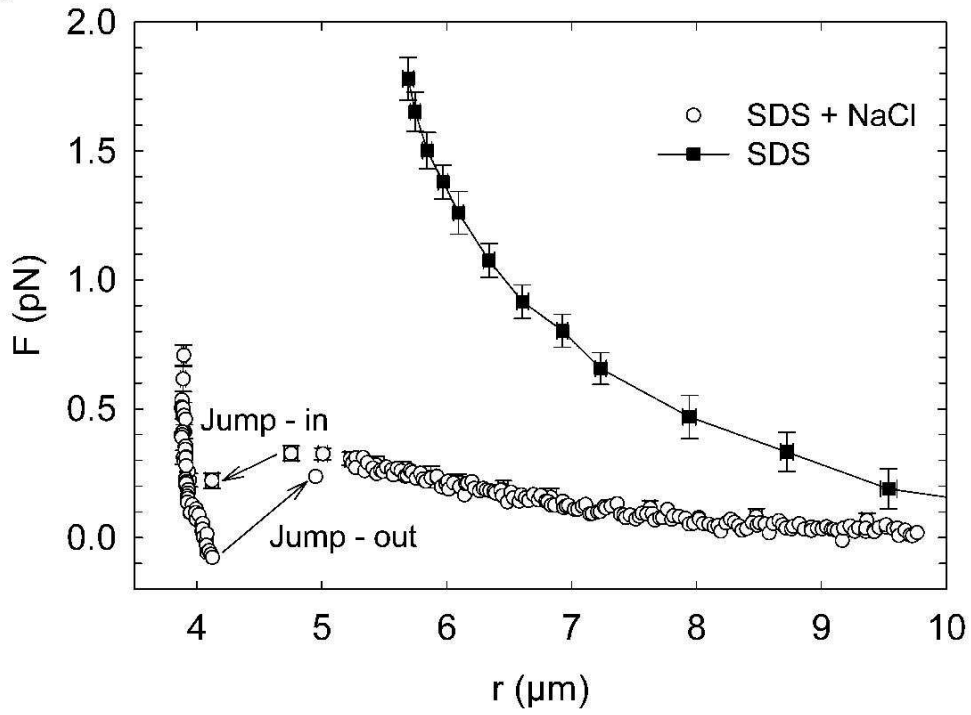

Figure 8: Measurement of the pair interaction force between between PS particles in 0.1mM SDS in the presence (open symbols) and absence (closed symbols) of 0.25M NaCl 108 minutes after spreading the particles.

Anisotropy of the interactions

From detailed studies of the aggregation kinetics and suspension structure, several features emerged that point to the role of anisotropic interactions [14]. These features are reproduced in aggregation experiments which correspond to a salt concentration of 0.1 M NaCl and 0.1 mM of SDS concentration, as discussed in the previous paragraph. Figure 9 shows two snapshots during the aggregation process of a monolayer with an average surface area coverage of approximately 0.30. The structures formed during the initial aggregation of the monolayer are predominantly linear aggregates. However, near completion of the aggregation process, the structure is rather dense. Typically, for systems with low SDS concentration in the presence of NaCl, the fractal dimension d_f is significantly higher than the one expected based on the DLCA kinetics (i.e. in the range between 1.45 and 1.58

versus the expected value, 1.44).

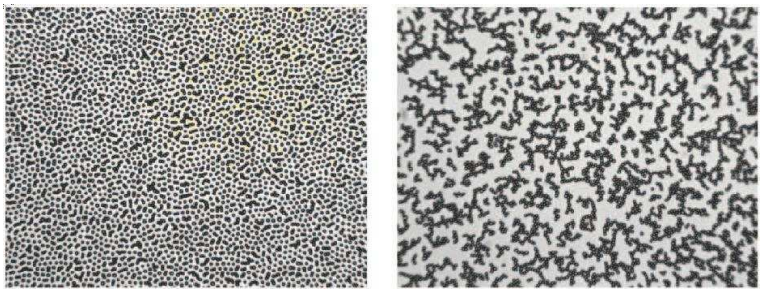

Figure 9: Snapshots of the microstructure during aggregation of an initially crystalline monolayer, destabilized by the addition of 0.1 mM SDS and 0.1 NaCl to the aqueous subphase. Left: structure formed after the initial aggregation. Right: structure formed after 1400 minutes. Scalebar 50 μm.

It is suggested that the linearity of the initial suspension structure upon aggregation is mainly caused by the anisotropy of the electrostatic interactions between the initial doublets and approaching single particles or doublets. To measure the magnitude of this interaction, different particle configurations were created as shown in figure 10. In the first arrangement, two particles are held using strong stationary traps, at a separation short enough that they form a dimer. A weak trap is then used to translate the third particle towards the dimer along the axis connecting the particle centers. The same dimer arrangement is used for the second experimental configuration, in which the third particle approaches the dimer orthogonal to the connecting axis.

The results for the anisotropic repulsive interaction for a dimer are shown in figure 10. In the case that the monomer approaches parallel to the dimer axis when the dimer particle separation is 3.5μm, the interaction is found to follow a power scaling with exponent -4, similar to the pair interaction. When approaching along the orthogonal axis a similar power-law dependence is found, suggesting that in both cases, the electrostatic dipole repulsion dominates. However, by comparing the prefactors from the power law fit of the interaction, we find that the dimer/particle interaction along the orthogonal axis is a factor

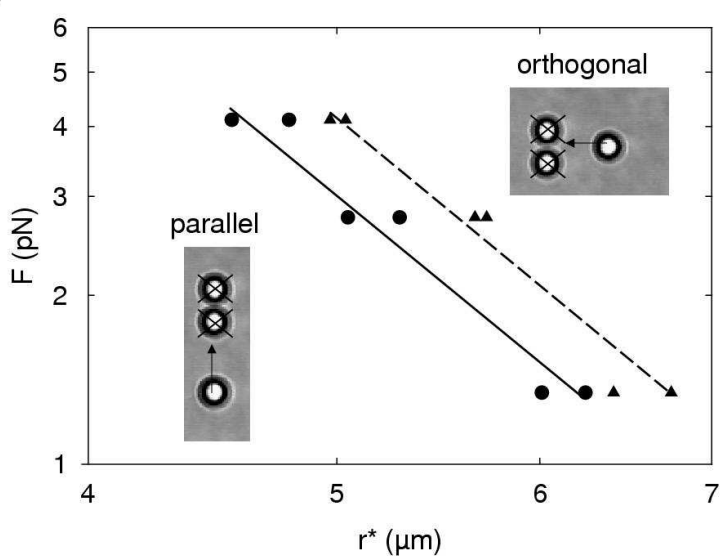

Figure 10: Measurements of the anisotropic interaction between a particle and a dimer 45±10 minutes after the PS particles were spread on the decane water interface with 0.5mM SDS in the aqueous phase. (a) Comparison of the interaction along the major axis of the dimer with a center-center separation of 3.5μm. (b) and the interaction along the minor axis of the same dimer.

of 1.3 times greater than the particle pair interaction. This explains why particles in aggregating system initially predominantly attach end-to-end, as the far-field energy barrier is smallest in this direction, yielding the highest probability for attachment.

The structures of the aggregating suspension, however, do not evolve linearly; they tend to densify and exhibit fractal dimensions which can be significantly higher than expected from the DLCA kinetics (1.47 to 1.58 depending on the compositional details the measured versus 1.44 expected). It has been argued previously that the anisotropy of the attractive capillary interaction plays an important role in this case. This has already been calculated for the case of gravitational induced capillary forces [36] or capillary forces induced by possible surface roughness [40]. The curvature of the meniscus of two interacting particles has two local minima occurring on either side of the doublet. The deformation in the

interstitial region can be complex, and depend on the wetting characteristics. However, in the present case the electro-capillarity can be expected to be much more important as compared to the gravitational forces [22, 37]. These electro-capillary interactions cannot be calculated assuming a superposition of the interfacial profiles, but can be approximated using a superposition of the electric field [39]. The range and magnitude of the electro-capillary forces depend on the charge density of the particles and the dielectric properties of the field. The effect of changing medium composition on the electro-capillary interaction can be expected to be very similar to the electrostatic repulsion and also the resulting spatial anisotropy would be similar but different in sign. The electro-capillary interaction can only compete with the electrostatic repulsion if $\epsilon_F = \mathcal{O}(1)$, see Eq. (7), i.e. if the total vertical electrostatic force on the colloid is of the order of γR. The contribution of possible charges on the oil side to the total vertical electrostatic force is small whereas the contribution of the charges on the water side can be large enough [37]. It has also been suggested that a non-uniform surface charge distribution leads to dipolar attractions [28]. Finally, the Van der Waals (VDW) attraction between particles will be affected by the wetting properties of the particles. The Hamaker constant of decane is 25% higher compared to water [19]. Pushing the particles into the oil phase hence weakens the VDW forces somewhat. The nature and anisotropy of these attractive interactions is not yet clear. Further work is required to elucidate how the changing wetting and charge density properties affect these interactions, possibly requiring an understanding of the multi-body effects.

In the present work, we evaluated experimentally whether the anisotropy in the attractive forces could indeed be responsible for rearrangements that lead to a more complex structure with a time-dependent aggregation. Using the optical traps, we assembled trimers two hours after spreading the particles on the decane-water interface with 1.0mM SDS in the aqueous phase. The maximum trapping force was approximately 20 pN. In figure

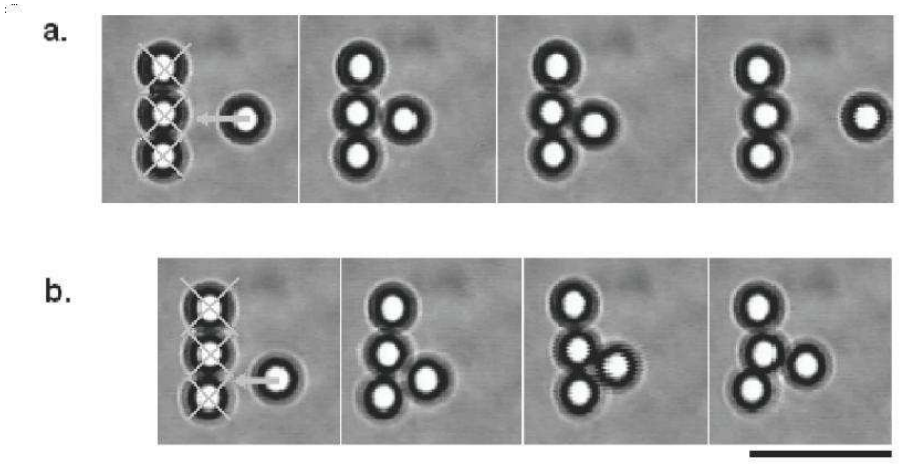

Figure 11: Approach of a monomer along the orthogonal to the axis of a trimer at the decane-water interface with 1.0mM SDS in the aqueous subphase. (a) The monomer is initially perfectly aligned with the center particle of the trimer. (b) This experiment was performed 1 minute later. The monomer is initially aligned with the region between the center and bottom particles of the trimer. In both cases $F_{max} > 20$pN. The scale bar is 10μm. Each time sequence goes from left to right.

11a, the approaching individual particle is perfectly aligned with the center particle of the trimer. We find that the trimer bends away from the approaching individual particle, and at a close separation, the individual particle begins moving downward, toward the region between the bottom two particles of the trimer. However, the repulsive barrier to aggregation becomes greater than the maximum trap strength, and the particle is released. At the same time, it appears that the triplet conformation becomes bent towards the right, the direction of the monomer's approach. One minute later, the approaching individual particle is aligned exactly between the two bottom particles of the trimer, where the capillary attraction is maximum. We observe that the aggregate rotates within the traps as the individual particle approaches due the repulsive interaction. However, the repulsive barrier is reduced by the capillary force and the traps are now strong enough to overcome the repulsion, and the individual particle aggregates to the center particle. In the system under investigation the repulsive forces are still considerable and the overall anisotropy

of the interaction is dominated by the repulsion, hence when the optical trap holding the fourth particle is removed, the particles reorient themselves to create a separation between the bottom particle and the newly attached particle.

Conclusions

Direct measurements of the pair-wise and multi-body interactions between polystyrene particles spread at the decane-water interface are reported. Using laser tweezers to measure the force between particles, the effect of changing the Debye screening length leads to a power law dependency of the interaction force. This suggests, contrary to earlier suggestions, that the charges on the water side may still contribute significantly. The power law exponent of 0.43 ± 0.04 is in good agreement with recent calculations, which account for charge renormalization at the particle surface. However, the absolute magnitude of the measured force is larger than what could be expected from only charges on the water side, hence it appears likely that charges on both oil and water side contribute to the repulsion. It is notable that the form of the repulsive interaction remains consistent with dipole–like behavior during the decrease of its magnitude upon adding salt. Likewise, introduction of SDS in the aqueous sub-phase was shown to result in a decrease in the repulsion between particles. Although treating SDS as a simple 1:1 electrolyte enables one to rationalize the observed initial decrease of the repulsion, the steady-state values of the contact angle and surface tension are dependent on surfactant concentration, and suggest an important role of the contact angle in controlling pair interactions. By trapping multiple particles, the multi-body interactions were also investigated. The stronger electrostatic interaction for single particles approaching orthogonal to an aggregate explain the tendency for linear structures to form in the early aggregation process of 2D suspensions. It was also found that in the near-field, the capillary interactions in the vicinity of aggregates are spatially anisotropic. As demonstrated in this work, the interactions between particles at the water-

oil interface in the presence of surfactants are significantly more complex; however, this also presents a unique opportunity to tailor the structure and rheology of interfacial suspensions by controlling the structure of suspension through the wetting properties of the particles and electrostatic interactions. In turn, this enables one to tailor the structure and stability of dispersed immiscible phases.

Acknowledgements

Basavaraj Madivala is acknowledged for his assistance in the gel trapping measurements. JV thanks research council of the K.U. Leuven for financial support through GOA-2003/06, and a research program of the Research Foundation-Flanders (FWO - Vlaanderen, project G.00469.05). EMF acknowledges support from NSF (CBET-0238689 and CBET-0553656). MO acknowledges funding through the Collaborative Research Centre SFB-TR6 of the German Research Council. This work was performed in the framework of a network of excellence SOFTCOMP (EU-6th framework).

References

[1] Binks, B.P; Horozov T.S. (Eds), *Colloidal Particles at Liquid Interfaces*, Cambridge University Press (2006).

[2] Ramsden W., Separation of solids in the surface-layers of solutions and 'Suspensions' (Observations on surface-membranes, bubbles, emulsions, and mechanical coagulation). Preliminary Account, *Proceedings of the Royal Society of London*, **72** (479): 156-164 (1903).

[3] Pickering, S.U., Emulsions, *Journal of the Chemical Society*, **91**: 2001-2021 (1907).

[4] Aveyard, R.; Binks, B.P.; Clint J.H., Emulsions stabilised solely by colloidal particles, *Advances in Colloid and Interface Science* **100**: 503-546 (2003).

[5] Dinsmore, A.D.; Hsu, M.F.; Nikolaides, M.G.; Marquez, M.; Bausch, A.R.; Weitz, D.A., Colloidosomes: Selectively permeable capsules composed of colloidal particles, *Science*, **298**: 1006-1009 (2002).

[6] Velev ,O.D.; Lenhoff, A.M.; Kaler, E.W., A class of microstructured particles through colloidal crystallization, *Science*, **287**:2240-2243 (2000).

[7] Manoharan V.N.; Elsesser M.T.; Pine D.J., Dense packing and symmetry in small clusters of microspheres, *Science* **301** (5632): 483-487 (2003).

[8] Vignati, E.; Piazza, R.; Lockhart, T.P., Pickering emulsions: Interfacial tension, colloidal layer morphology, and trapped-particle motion", *Langmuir* **19**: 6650-6656 (2003)

[9] Midmore, B.R., Synergy between silica and polyoxyethylene surfactants in the formation of O/W emulsions", *Colloids and surfaces A -physicochemical and engineering aspects* **145** : 133-143 (1998).

[10] Zahn, K.; Lenke, R.; Maret, G., Two-stage melting of paramagnetic colloidal crystals in two dimensions,*Physical Review Letters* **82**: 2721-2724 (1999).

[11] Robinson, D.J.; Earnshaw, J.C., Experimental-study of colloidal aggregation in 2 dimensions. 1. Structural aspects; *Physical Review A*, **46**: 2045-2054 (1992).

[12] Robinson, D.J.; Earnshaw, J.C., Experimental-study of colloidal aggregation in 2 dimensions.2. Kinetic aspects; *Physical Review A* **46**: 2055-2064 (1992).

[13] Hansen, P.H.F.; Bergstrom, L., Perikinetic aggregation of alkoxylated silica particles in two dimensions, *Journal of Colloid and Interface Science* **218**: 77-87 (1999).

[14] Reynaert S.; Moldenaers P.; Vermant, J., Control over colloidal aggregation in monolayers of latex particles at the oil-water interface *Langmuir*, **22**: 4936-4945 (2006).

[15] Loudet, J.C.; Alsayed, A.M.; Zhang, J.; Yodh, AG, Capillary interactions between anisotropic colloidal particles, *Physical Review Letters*, **94**: Art. No. 018301 (2005)

[16] Basavaraj, M.G.; Fuller, G.G.; Fransaer, J.; Vermant, J.; Packing, flipping, and buckling transitions in compressed monolayers of ellipsoidal latex particles, *Langmuir*, **22**: 6605-6612 (2006).

[17] Stancik, E.J.; Gavranovic, G.T.; Widenbrant, M.J.O.; Laschitsch, A.T.; Vermant, J.; Fuller, G.G.; Structure and dynamics of particle monolayers at a liquid-liquid interface subjected to shear flow, *Faraday Discussions*, **123**: 145-156 (2003).

[18] Hoekstra H., Vermant J., Mewis J., Fuller G.G.; Flow-induced anisotropy and reversible aggregation in two-dimensional suspensions, *Langmuir* **19**: 9134-9141 (2003).

[19] Israelachvili, J., *Intermolecular and surface forces*, Academic Press, 2nd Ed. (1991)

[20] Russel, W.R.; Saville D.A.; Schowlater W.R., *Colloidal Dispersions*, Cambridge university press (1989)

[21] Aveyard, R.; Clint, J.H.; Nees, D.; Paunov, V.N. Compression and structure of monolayers of charged latex particles at air/water and octane/water interfaces *Langmuir*, **16**: 1969-1979 (2000).

[22] Frydel, D.; Oettel, M.; Dietrich, S.; Charge renormalization effects in the electrostatic interactions of colloids at interfaces, *Phys. Rev. Lett* in press, arXiv:0705.1463v1 (2007).

[23] Fernández-Toledano, J.C.; Moncho-Jordá, Martínez-López F.; Hidalgo-Alvarez R., Theory for interactions between particles in Monolayers, Ch.3 in *Colloidal Particles at Liquid Interfaces*, Binks, Horozov (Eds) Cambridge University Press (2006).

[24] Ruiz-Garcia, J.; Gamez-Corrales, R.; Ivlev, B.I.; Formation of two-dimensional colloidal voids, soap froths, and clusters, *Physical Review E*, **58** (1): 660-663 (1998).

[25] Mejia-Rosales, S.J.; Gamez-Corrales, R.; Ivlev, B.I.; Ruiz-Garcia, J., Evolution of a colloidal soap-froth structure, *Physica A-Statistical Mechanics and its Applications*, **276** (1-2): 30-49 (2000).

[26] Ghezzi, F.; Earnshaw, J.C., Formation of meso-structures in colloidal monolayers, *Journal of Physics-Condensed Matter*, **9**: L517-L523 (1997).

[27] Ghezzi, E.; Earnshaw, J.C.; Finnis, M.; McCluney, M.; Pattern formation in colloidal monolayers at the air-water interface, *Journal of Colloid and Interface Science*, **238**: 433-446 (2001).

[28] Chen W.; Tan S.S.; Huang Z.S.; Ng T.K.; Ford W.T.; Tong P.; Measured long-ranged attractive interaction between charged polystyrene latex spheres at a water-air interface *Physical review E* **74**: Art. No. 021406 (2006).

[29] Aveyard, R.; Clint, J.H.; Nees, D.; Paunov, V.N.; Structure and Collapse of Particle Monolayers under Lateral Pressure at the Octane/Aqueous Surfactant Solution Interface, *Langmuir*, 16, 8820-8828 (2000).

[30] Pieranski, P., Two-Dimensional Interfacial Colloidal Crystals, *Physical Review Letters*, **45**, 569-572 (1980).

[31] Aveyard, R.; Binks, B.P.; Clint, J.H.; Fletcher, P.D.I.; Horozov, T.S.; Neumann, B.; Paunov, V.N.; Annesley, J.; Botchway, S.W.; Nees, D.; Parker, A.W.; Ward, A.D.; Burgess, A.N., Measurement of long-range repulsive forces between charged particles at an oil-water interface, *Physical Review Letters*, **88**): Art. No. 246102 (2002).

[32] Hurd A.J.; The electrostatic interaction between interfacial colloidal particles, *J. Phys A-Mathematical and general*, **18**: 1055-1060 (1985).

[33] Moncho-Jordá, Martínez-López F.; Gonzalez, A.E.; Hidalgo-Alvarez, R.,Role of long-range repulsive interactions in two-dimensional colloidal aggregation: Experiments and simulations, *Langmuir*, **18**: 9183-9191 (2002).

[34] Sun, J.Z., Stirner, T., Molecular dynamics simulation of the surface pressure of colloidal monolayers, *Langmuir*, **17**: 3103-3108 (2001).

[35] Kralchevsky P.A; Nagayama,K., Capillary Forces between Colloidal Particles *Langmuir*, **10**, 23-36 (1994)

[36] Kralchevsky P.A; Nagayama, K., Capillary interactions between particles bound to interfaces, liquid films and biomembranes, *Advances in Colloid and Interface Science* **85**, 145-192 (2000).

[37] Oettel M.; Dominguez A.; Dietrich S.; Attractions between charged colloids at water interfaces, *Journal of Physics-Condensed Matter*, **17**: L337-L342 (2005).

[38] Danov K.D., Kralchevsky P.A., Electric forces induced by a charged colloid particle attached to the water-nonpolar fluid interface, *Journal of Colloid and Interface Science* **298**: 213-231 (2006).

[39] Dominguez A.; Oettel M.; Dietrich S.; Capillary-induced interactions between colloids at an interface *Journal of Physics-Condensed Matter*, **17**: S3387-S3392 (2005).

[40] Stamou D., Duschl C., Johannsmann D., Long-range attraction between colloidal spheres at the air-water interface: The consequence of an irregular meniscus, *Physical Review E* **62**: 5263-5272 (2000).

[41] Vassileva N.D.; van den Ende D.; Mugele F.; Mellema J., Capillary forces between spherical particles floating at a liquid-liquid interface, *Langmuir* **21**: 11190-11200 (2005).

[42] Pantina, J.P.; Furst, E.M., Directed assembly and rupture mechanics of colloidal aggregates, *Langmuir*, 20 (10): 3940-3946 (2004).

[43] Faucheux, L.P., Stolovitzky G., Libchaber A., Periodic forcing of a brownian particle *Physical Review E* **51**: 5239-5250 (1995).

[44] Paunov, V.N., Novel method for determining the three-phase contact angle of colloid particles adsorbed at air-water and oil-water interfaces *Langmuir* **19**: 7970-7976 (2003).

[45] Nakagaki, M., Yokoyama, S., Acid-catalyzed hydrolysis of sodium dodecyl-sulfate, *J. Pharmaceutical Sci.* **74**: 1047-1052 (1985).

[46] Turner, S.F., Clarke, S.M., Rennie, A.R., Thirtle, P.N., Cooke P.J., Li, Z.X., and Thomas, R.K., Adsorption of sodium dodecyl sulfate to a polystyrene/water interface studied by neutron reflection and attenuated total reflection infrared spectroscopy *Langmuir* **15** (4): 1017-1023 (1999).

[47] Benjamin, I., Molecular structure and dynamics at liquid-liquid interfaces, *Annual Review of Physical Chemistry*, **48**: 407-451 (1997).

TABLE OF CONTENTS GRAPH